

www.acsmaterialsletters.org

# Adsorption Mechanism of Perfluorooctanoate on Cyclodextrin-Based Polymers: Probing the Synergy of Electrostatic and Hydrophobic Interactions with Molecular Dynamics Simulations

Aditya Choudhary, Dengpan Dong, Marina Tsianou, Paschalis Alexandridis, and Dmitry Bedrov\*



**Cite This:** ACS Materials Lett. 2022, 4, 853–859



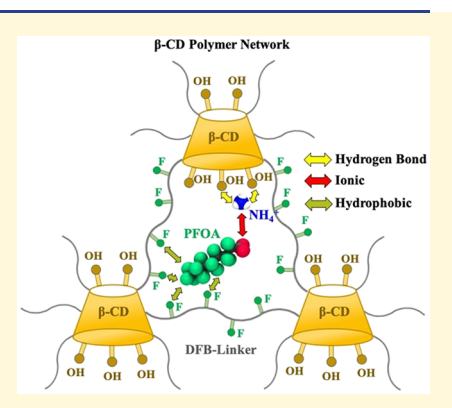
**ACCESS** 

Metrics & More

Article Recommendations

Supporting Information

ABSTRACT: Contamination of natural water resources by per- and polyfluorinated alkyl substances (PFAS) has affected millions of people around the world and emphasized the need for development of novel and effective adsorbent materials. We demonstrate how atomistic molecular dynamics (MD) simulations can be used to provide molecular scale insight into the role of electrostatic and hydrophobic interactions on the adsorption of the perfluorooctanoate (PFOA) surfactant, a prominent longer-chain PFAS, on a polymer-based network in water. Specifically, the adsorption of ammonium perfluorooctanoate salt has been investigated on the  $\beta$ -cyclodextrin (CD) network cross-linked with decafluorobiphenyl linkers as an example of an absorbent material that has already demonstrated efficient PFAS adsorption. Examination of pairwise interactions reveals the importance of the dual pronged adsorption mechanism involving both electrostatic and hydrophobic interactions. The adsorption of ammonium counterions on the CD segments



facilitates attraction of the anionic headgroup of the PFOA surfactant, while fluorinated linkers provide an additional hydrophobic attraction for the PFOA tail as well as higher affinity of the network toward PFOA in comparison with hydrocarbons. These competing interactions result in PFOA adsorption primarily outside of the CD cavity with the PFOA tail mostly interacting with fluorinated linkers. We demonstrate that simulations using "what if" scenarios are a powerful approach to infer the role of different interactions in the adsorption of PFAS.

er- and polyfluoroalkyl substances (PFASs) are known as "forever chemicals" owing to their thermodynamically stable C-F bond. Such molecules are often found in natural water and demonstrate high persistence, bioaccumulation,<sup>2</sup> and toxicity,<sup>3</sup> that have triggered major health and environmental concerns. 4,5 Among 9,500 different types of PFAS, perfluorooctanoic acid and perfluorooctanesulfonic acid are among primarily identified pollutants that have been extensively used in the production of firefighting foams, nonstick cookware, packaging materials, waterproof clothing, and fluoropolymers. 6,7 Only in the United States, they have been found in water bodies at more than 1400 sites which are serving up to 110 million people.8 The U.S. Environmental Protection Agency has issued a health advisory level of 70 ng/L for the combined concentration of PFOA and PFOS in drinking water.5

Many techniques based on oxidation, 10 photochemical reduction, 11 and electrochemical degradation 12 have been

proposed to break the strong C–F bond. However, these methods are expensive and require extreme reaction conditions and high energy. Moreover, degrading such fluorinated pollutants generates byproducts with unknown toxicity. Therefore, a more practical approach would be first to sequester these compounds out of the environment and then apply the above-mentioned degradation methods. For the filtration, adsorption is proved to be a versatile and cost-effective technique for PFAS removal. Many adsorbents consisting of granular activated carbon (GAC), <sup>14</sup> mineral

Received: February 20, 2022 Accepted: March 29, 2022 Published: April 4, 2022





surfaces, <sup>15</sup> anion exchange resins, <sup>16</sup> metal—organic frameworks (MOFs), <sup>17</sup> and organic polymers <sup>18</sup> have been investigated. Conventionally, GAC is regarded as one of the efficient and affordable filtering materials but shows a poor affinity for PFAS molecules, which makes it ineffective at environmentally relevant concentrations, <sup>19</sup> and also, the regeneration of PFAS-loaded GAC is an energy-intensive process. <sup>20</sup> Therefore, the design of new materials with appropriate host—guest compatibility is crucial for the successful removal of these fluorinated molecules from the aqueous environment.

Several strategies for the design of polymer- and oligomerbased adsorbent materials with tailored selectivity for fluorinated pollutants have been recently proposed.<sup>21-24</sup> It has been suggested that materials incorporating macrocyclic chemistry can serve this purpose owing to their potential for controlling molecular recognition and binding ability.<sup>25-27</sup> One of the considered macrocyclic hosts is  $\beta$ -cyclodextrin ( $\beta$ -CD), composed of seven glucose units, which displays a strong association constant of  $5.0 \times 10^5$  and  $7.0 \times 10^5$  M<sup>-1</sup> for the 1:1 host-guest complexes  $\beta$ -CD/PFOA and  $\beta$ -CD/PFOS, respectively.<sup>28</sup> NMR measurements provided evidence that in aqueous solutions PFOA molecules can insert inside the more hydrophobic interstitial cavity of  $\beta$ -CD. <sup>29,30</sup> These motivated Dichtel and Helbling to propose a novel CD-based crosslinked network that can function as an adsorbent material for PFAS removal from water.<sup>31–35</sup> Interestingly, the adsorption rate constant of such polymers was found to be 15 to 200 times higher compared to non-cross-linked CDs and activated carbon. In these networks, CDs were cross-linked with rigid aromatic segments to form a mesoporous network material with high surface area. It was shown that variation in crosslinker chemistry allowed tuning of the adsorption capacity, kinetics, and selectivity toward different PFAS. For example, a network with tetrafluoroterephthalonitrile (TFN) linkers displayed an excellent removal rate for cationic and neutral organic micropollutants; however, due to the presence of a few anionic phenolate groups, which were introduced during the polymerization process, it showed a poor affinity for PFOA.<sup>36</sup> The influence of cross-linkers on PFAS uptake by CD-based networks was compared for decafluorobiphenyl (DFB), epichlorohydrin (EPI), and 2-isocyanatoethyl methacrylate (IEM) and many other cross-linkers with varying density.<sup>34</sup> Although the networks with perfluorinated aromatic (DFB) linkers exhibited a larger negative zeta potential, they proved to be a better performing adsorbent. Incorporation of aminebased cross-linkers showed an even better performance for PFAS adsorption.<sup>3</sup>

While the above-discussed experimental data show great promise for cyclodextrin polymer (CDP) adsorbents, several important questions regarding adsorption mechanisms remain open. For example, experiments suggest that not just the surface charge but the microenvironment around the cyclodextrin plays a crucial role in the adsorption process. But, is it necessary to have fluorinated linkers in order to achieve high adsorption and selectivity of PFAS? Also, what is the role of cyclodextrin molecules in the adsorption of PFAS? While some measurements show that adsorption capacity correlates with the molar density of CDs, others show that variation in crosslinker chemistry leads to a significant change in adsorption capabilities. 34,38 Which interactions (e.g., hydrophobic, electrostatic, etc.) play the key role in defining the affinity of pollutants to adsorbent? In this Letter, we demonstrate how these questions and details of adsorption mechanisms at the

molecular scale, which are difficult to assess through experiments, can be investigated using atomistic MD simulations.

For this demonstration, we investigated ammonium perfluorooctanoate (PFOA) salt, as a model representative of long-tail PFAS, on a two-dimensional network of  $\beta$ -CDs crosslinked with decafluorobiphenyl (DFB) (see Figure 1).

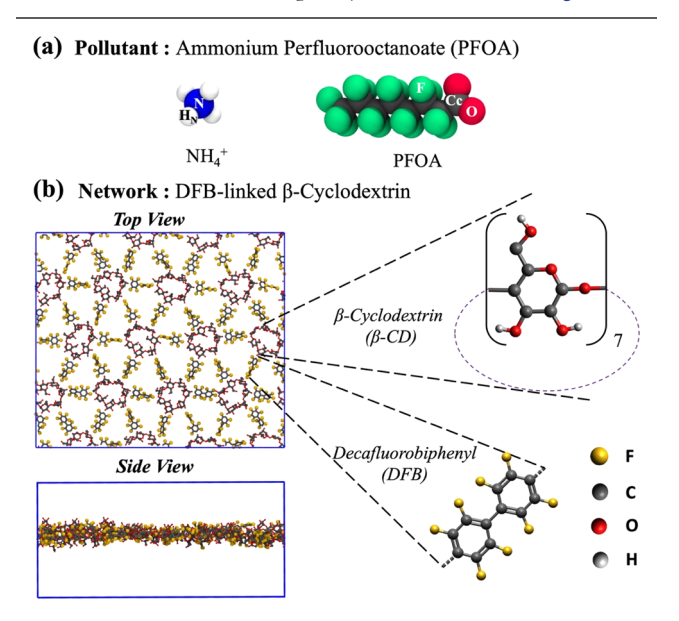


Figure 1. (a) Chemical structure of the PFAS pollutant (ammonium (NH<sub>4</sub><sup>+</sup>) perfluorooctanoate (PFOA)) considered in this work. (b) Top and side views of the decafluorobiphenyl (DFB)-linked  $\beta$ -cyclodextrin ( $\beta$ -CD) network immersed in water. Water molecules are not shown.

Contrary, to the common belief that insertion of the fluorinated tail inside the CD cavity is the primary mechanism for PFOA adsorption in these networks, we find that the crosslinker is playing a major role in defining the interactions/ adsorption of PFOA. Simulations reveal that a combined effect of (i) strong polar interactions between the PFOA headgroup, ammonium counterion, and hydroxyl groups of CD and (ii) strong hydrophobic attraction between the PFOA tail and fluorinated linker are the primary mechanisms for efficient adsorption of PFOA surfactants. Furthermore, the computational methodology enables us to artificially introduce chemical modifications in the network, such as replacing fluorinated linkers with hydrogenated or biasing specific interactions to assess the role of pairwise interactions among different components of the system. This helps to elucidate the role of CDs, linkers, and counterions during the pollutant removal process. The adsorption mechanisms deduced from this molecular scale study reveal a complex interplay of interactions between species, which are likely to be relevant to other adsorbents considered for PFAS removal. This approach can be employed for the molecular design of materials with high selectivity and removal efficiency of fluorinated pollutants.

All simulations were conducted using an in-house developed MD package with a nonpolarizable version of the Atomistic Polarisable Potential for Liquid, Electrolytes, and Polymers (APPLE&P) force field.<sup>39</sup> This version of the force field has been previously used in simulation of PFOA and GenX aqueous solutions, 40-42 which proved to be in excellent agreement with the experimental results. The missing

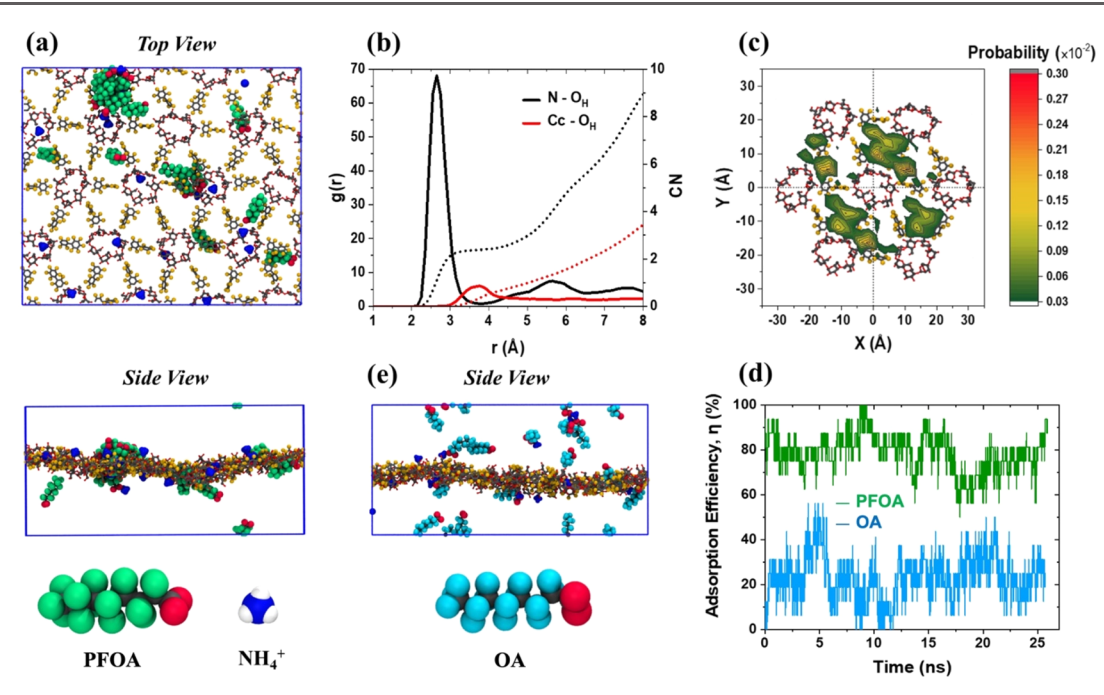


Figure 2. a) Top and side views of the DFB-linked  $\beta$ -CD network with PFOA and ammonium ions highlighted. (b) The radial distribution function (g(r)) and the corresponding coordination number (CN) between the N of NH<sub>4</sub><sup>+</sup> and hydroxyl O atoms of CD  $[N-O_H]$  and between the double-bonded carbon atom (Cc) of the PFOA headgroup and hydroxyl O atoms of CD  $[Cc-O_H]$ . (c) Two-dimensional probability distribution of locations of PFOA ions' center-of-mass adsorbed to the network (i.e., located within the 8.0 Å layer from the plane of the network) relative to the center-of-mass of the CD ring. (d) Time evolution of adsorption efficiency for PFOA and ammonium octanoate (OA). (e) Side view of the final snapshot of the DFB-linked  $\beta$ -CD network with OA as the pollutant.

parameters to describe CD and DFB linkers were parametrized against quantum chemistry calculations (see the Supporting Information for parameters). All chemical bond lengths were constrained using the SHAKE algorithm. The long-range electrostatic interactions were computed using the Ewald summation method, and a cutoff distance of 15 Å was incorporated for both van der Waals and the real part of electrostatic interactions. A multiple time step approach was utilized with the shortest time step of 0.5 fs for bonds, bends, and improper torsional motions, a medium time step of 1.5 fs for dihedrals and short-range (<8.0 Å) nonbonded interactions, and a larger time step of 3 fs for long-range (>8.0 Å) nonbonded interactions and the reciprocal part of Ewald summation.

A three-dimensional periodic simulation box contained a 2D periodic network comprised of 16  $\beta$ -CDs and 48 DFB linkers, as illustrated in Figure 1. The network was solvated with an aqueous solution containing 12,000 water molecules and 16 PFOA/NH<sub>4</sub><sup>+</sup> pairs. The selected 3:1 ratio of DFB:β-CD corresponds to a network configuration that experimentally showed good adsorption efficiency.<sup>32</sup> Each DFB linker is shared between two CD rings, where one end is connected covalently, while the other end is attached through a harmonic bond of length 2.0 Å with a stiffness of 100 kcal/mol/Å<sup>2</sup>. The overall concentration of PFOA in the system corresponded to 65.5 mM, which is above its critical micelle concentration (25 mM).<sup>44</sup> While the concentration of PFAS contamination in bulk water is typically much lower, at the surface and the vicinity of the adsorbent material, one can expect the pollutant concentration to be much higher once the material has been exposed to the solution. The initial dimensions of the simulation cell were shrunk to an expected density over 30 ps at 300 K. Initially, PFOA, NH<sub>4</sub><sup>+</sup>, and water molecules were

randomly distributed in the solution. Equilibration runs over 3 ns were followed by production runs over 40 ns in the NPT ensemble. The cell dimension in the direction perpendicular to the network was close to 5 nm which is large enough to minimize the influence of self-replicas due to periodic boundary conditions.

First, we studied the adsorption process of the PFOA pollutant on the DFB-linked  $\beta$ -CD network. Figure 2a illustrates the top and side views of the DFB-linked CD network exposed to the PFOA-containing solution. PFOA and NH<sub>4</sub><sup>+</sup>, highlighted in green and blue, respectively, are mostly adsorbed on the network. Simulations show that 95% of ammonium ions are bound to the network, and about 78% of PFOA ions are adsorbed with their center-of-mass being within the 8.0 Å layer next to the network (Figure S2). Moreover, many adsorbed PFOA ions form small clusters on the surface. Figure 2b shows radial distribution functions, g(r), i.e., the function characterizing the pairwise correlations and interactions, between the N atom of NH<sub>4</sub><sup>+</sup> with the hydroxyl oxygen atom (O<sub>H</sub>) of CD [N-O<sub>H</sub>] and between the doublebonded carbon atom (Cc) of the PFOA headgroup with hydroxyl oxygen [Cc-O<sub>H</sub>]. The high intensity first peak for the N-O<sub>H</sub> correlation indicates the strong electrostatic interaction (hydrogen bonding) of ammonium with hydroxyl groups of CD. The coordination number (CN) of 2.4 (within the first coordination shell of 3.75 Å) suggests that each NH<sub>4</sub><sup>+</sup> typically has direct contact with two or three -OH groups of CD. The strong interaction between the ammonium cation and CDs is consistent with the snapshot shown in Figure 2a, where NH<sub>4</sub><sup>+</sup> ions are found to be adsorbed near the circumference of CD. The Cc-O<sub>H</sub> correlation, on the other hand, shows a comparatively weak correlation between the PFOA headgroup and hydroxyls of CD, despite also having the

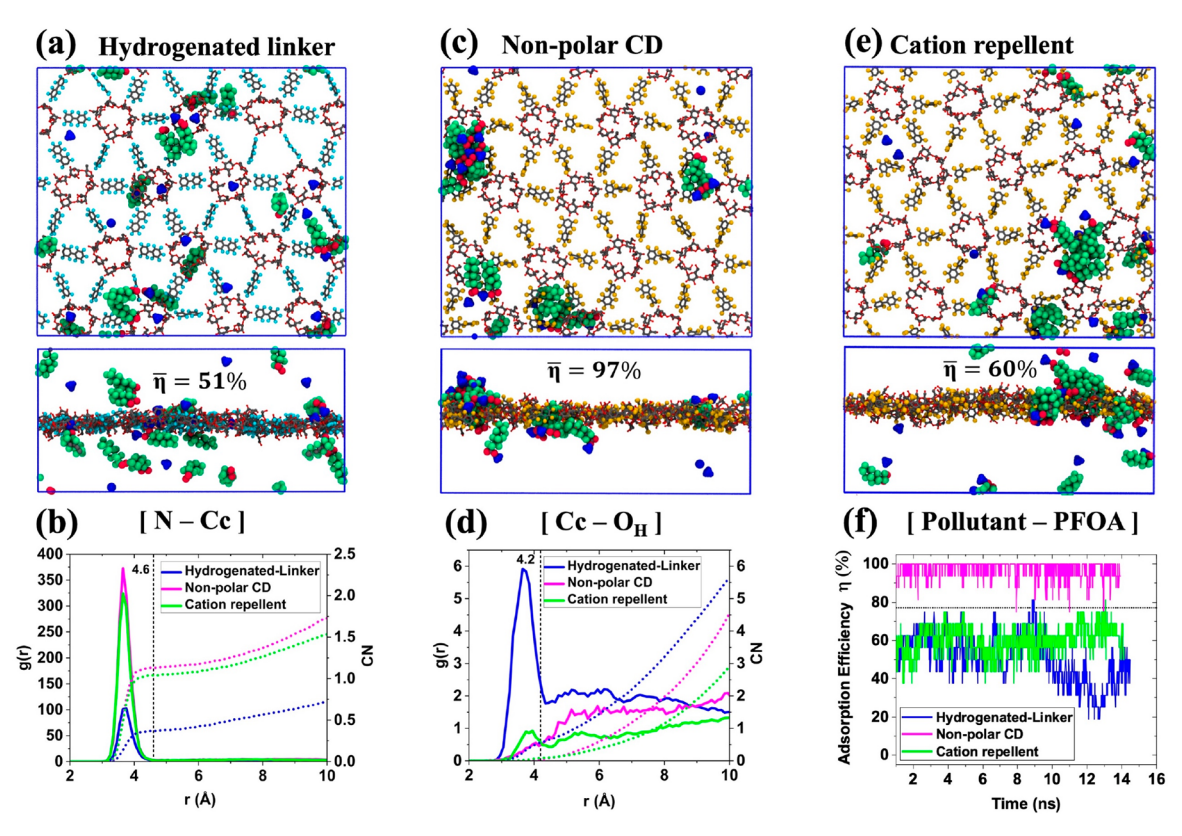


Figure 3. (a), (c), and (e): Top and side views of the equilibrated biphenyl-linked cyclodextrin (CD) network, network with nonpolar CD, and cation-repellent network, respectively. The average adsorption efficiency  $(\bar{\eta})$  is reported in side view panels. (b) and (d): The radial distribution function (g(r)) and the corresponding coordination number (CN) between the N of the NH<sub>4</sub><sup>+</sup> ion and the headgroup of PFOA [N-Cc] and between the double-bonded carbon atom (Cc) of the headgroup of PFOA and the hydroxyl O atom [Cc-O<sub>H</sub>], respectively. (f) Adsorption efficiency  $(\eta)$  of the PFOA pollutant as a function of the simulation time for various networks with biased interactions.

possibility to form hydrogen bonds. Within a 4.2 Å coordination shell, the Cc atom of PFOA has on average 0.6 hydroxyls in direct contact. Finally, the analysis of [N–Cc] correlations (Figure S3) showed that, on average, at any given time about 50% of PFOA head groups are associated with ammonium counterions.

From simulations, we can straightforwardly assess the preferred positions in the network for PFOA adsorption. Figure 2c shows a two-dimensional probability distribution for finding the center-of-mass of PFOA in the 8.0 Å layer next to the network and relative to the CD ring position (see Figure S4 for detailed criteria). The PFOA molecules satisfying this condition have multiple atom-atom direct contacts with the network atoms and, hence, can be considered as adsorbed. The most probable regions of finding PFOA on the network (i.e., red and yellow regions in the distribution) lie within the cavities formed by the DFB linkers and not within the interstitial cavities of CD. This is different from what was previously assumed based on observed PFAS-CD complexation in aqueous solutions. <sup>29,45,46</sup> At the same time, it is consistent with recent literature that observed a drastic effect of cross-linkers in CD-based networks on the adsorption of PFOA (and another PFAS), 21,34,47 which can be indicative that the primary adsorption mechanism does not involve PFAS-CD inclusion complex formation. Through MD simulations, we have obtained the potential of mean-force for inserting a single PFOA ion from the bulk water into the  $\beta$ -CD cavity. Figure S5 shows that there is a 2.2 kcal/mol free energy barrier for such an insertion. Instead, pores formed by linkers provide the appropriate environment that has a strong affinity toward PFOA fluorinated tails and controls the adsorption of these pollutants.

In addition to adsorption efficiency of the network toward PFAS compounds, it is extremely important to make sure that other organic matter present in water would not interfere with the adsorption capacity of the membrane. To test this, we have conducted simulations of the same network but replaced the PFOA pollutant with its hydrogenated analogue, *i.e.*, ammonium octanoate (OA). Figure 2d shows that the efficiency of adsorption dropped from 78% to 23%, confirming the higher affinity of a CD-based DFB cross-linked network toward fluorinated molecules. A side view of the equilibrated system with OA surfactants (Figure 2e) clearly captures the poor adsorption behavior of hydrogenated pollutants.

One of the advantages of MD simulations is the ability to investigate the "what if" scenarios in which we artificially adjust interactions or chemical structures of selected component(s) without changing any other parameters of the system. This allows attaining further insight into the role that each interaction and component plays in the adsorption mechanism of PFOA. In the following sections, we investigate the role of different components of the network.

In order to understand the importance of the fluorinated linker, we investigate a network with biphenyl (BP) linkers, which is the hydrogenated counterpart of the DFB linker (Figure S6), while keeping all other components of the system the same. This system will be referred to as the "hydrogenated linker" for further discussion. The top and side views of a

typical snapshot (Figure 3a) of such a system clearly show a noticeable change in the adsorption state. First, a significant reduction is observed in the number of PFOA molecules adsorbed on the surface, just 50% of PFOA are within 8.0 Å from the "hydrogenated linker" network, which clearly indicates the importance of fluorinated linkers. The PFOA surfactants that are adsorbed on the network have their fluorinated tails oriented primarily perpendicular to the network, indicating no preferential hydrophobic interaction with BP linkers. The ammonium ions that are bound to the network surface strongly correlate with CD hydroxyls and the head groups of PFOA. Analysis of the g(r) and coordination numbers for [N-Cc] (Figure 3b), [Cc-O<sub>H</sub>] (Figure 3d), and [N-O<sub>H</sub>] (Figure S7) correlations showed very similar results as for the original system, which is not surprising as those interactions would not be affected by changing the linker structure. Also, there is no association of PFOA in the solution, despite the fact that the overall concentration of PFOA is above its CMC. We believe that the strong adsorption of ammonium ions onto CDs interferes with their ability to facilitate the screening of electrostatic interactions upon PFOA self-assembly into micelles. While a significant fraction of PFOA anions is still associated with ammonium cations, the anchoring of cations with CDs does not allow those PFOA/  $\mathrm{NH_4}^+$  complexes to associate.

It becomes clear from the above discussion, that the hydroxyl groups of CD are primarily interacting with NH<sub>4</sub><sup>+</sup> and PFOA ions, and hence, it is crucial to understand their role during the adsorption process. To do that, we conducted a simulation where the dipole moments of all -OH groups on CD were scaled to zero (referred to as the "nonpolar CD" system). The top and side views of the final snapshot of this system (Figure 3c) as well as the analysis of radial distribution functions (Figure S7) suggest the absence of strong interactions between NH<sub>4</sub><sup>+</sup> and cyclodextrin, since reducing its polarity makes CD incapable of forming any hydrogen bonds that were observed in the original system. The snapshot clearly shows that the majority of ammonium ions (blue) remains in bulk water and stays away from the network. Similarly, the interaction between PFOA head groups and CD hydroxyls is also weakened significantly (Figure 3d). On the other hand, a sharp peak in the [N-Cc] pair correlation (Figure 3b) confirms an enhanced interaction between NH<sub>4</sub><sup>+</sup> and PFOA. After turning off the polarity of hydroxyl groups in the "nonpolar CD" system, the surface of the CD also becomes hydrophobic, which can be confirmed by the g(r) and CN between the O<sub>H</sub> and O<sub>w</sub> (oxygen atom of a water molecule) presented in Figure S8a. In order to realize the extent of hydrophobicity of the CD surface, the g(r) and CN of  $O_w$  are compared around the F<sub>DFB</sub> (fluorine atom of DFB linker) and O<sub>H</sub> of CD (Figure S8b). Interestingly, both F<sub>DFB</sub> and O<sub>H</sub> display a similar feature with a comparable coordination number, confirming that the CD surface in the "nonpolar CD" system acts chemically analogous to a DFB linker.

Figure 3c shows that almost all of the PFOA ions are adsorbed at the network. The time-average adsorption efficiency of the "nonpolar CD" network is about 97% which is even higher compared to the unaltered system (Figure 3f). Such an enhancement in the removal efficiency is achieved owing to an effective increase of the apolar surface area of the network. Examining the sites for PFOA adsorption through 2D probability distribution (Figure S9b) reveals that, in this system, the majority of PFOA ions adsorbs in the cavity

formed by DFB linkers, while a small fraction of it is on CD. Making CDs more hydrophobic in this system increases the adsorption efficiency; however, we believe that it will also decrease the network wettability and interfere with the ability of water to penetrate through such a network.

Next, we examine the role of the counterion (in our case, NH<sub>4</sub><sup>+</sup>) in the adsorption mechanism of PFOA which is rarely addressed in the literature. To understand the importance of a strong NH<sub>4</sub><sup>+</sup>/CD interaction during the adsorption of a PFOA ion, we created a system where the repulsion between ammonium and hydroxyl groups of CD was artificially increased such that they cannot approach closer than 3.2 Å to each other (Figure S10), while keeping other interactions intact. This effectively prevents the adsorption of NH<sub>4</sub><sup>+</sup> on the network, yet the CDs remain hydrophilic for all other components. This system is referred to as a "cation repellent". A typical snapshot of such a system is given in Figure 3e and shows that the majority of the ammonium ions is in the bulk solution. In this system, a sharp peak in g(r) for the [N-Cc] pair (Figure 3b) confirms that the interaction between the PFOA headgroup and NH<sub>4</sub><sup>+</sup> remains strong, whereas a significant reduction in the interaction between PFOA head groups and CD hydroxyls can be seen in Figure 3d. Although we introduced the repulsion term only between NH<sub>4</sub><sup>+</sup> and CD hydroxyls, a decrement in the PFOA and CD interaction compared to the original system as well as the network with the "hydrogenated linker" suggests that the PFOA and CD interactions were mediated through the presence of ammonium ions. As a result, in the system where  $NH_4^+$  is not adsorbing onto the network, the removal efficiency drops to 60%, indicating that the presence of DFB linkers alone is not sufficient to provide strong partitioning of fluorinated surfactants to the network. The adsorption of cations on CDs facilitates the adsorption of PFOA on the network by providing sites with positive charge density for the headgroup of an anionic pollutant to interact with. Note that originally, introduction of CDs to the network was thought to facilitate their direct hydrophobic interaction with PFAS tails, but the counterion adsorption on CDs has changed the mechanism and the role CDs are playing in the PFOA adsorption by the network. A similar influence of counterions has also been observed in ionic gels, where the presence of quaternary ammonium groups in the adsorbent was found to augment the removal efficiency of PFAS compared to a charge neutral adsorbent. 23,48,49

In summary, in this work, we demonstrate how atomistic MD simulations can be used to study the role of different interactions and adsorption mechanisms of PFAS pollutants on CD-based networks. Using a specific example of ammonium perfluorooctanoate as a pollutant and a  $\beta$ -cyclodextrin network cross-linked with decafluorobiphenyl linkers as a model adsorbent polymer, we conducted simulations with several "what if" scenarios of biased interactions and chemical structures to assess the role of CDs, linkers, and counterions in the adsorption mechanism. The analysis of molecular scale interactions reveals that the mechanism of adsorption of PFOA pollutants on the CD-based network is governed by two primary factors. First, the adsorption of ammonium ions on CD segments of the network gives rise to strong ionic interactions between the headgroup of the pollutant and the network. While the network is not ionic by design, the strong interaction of polar segments (i.e., CDs) with cations effectively renders this network similar to those where cationic

groups are incorporated into the network chains. Second, the presence of fluorinated linkers creates fluorophilic pockets for the fluorocarbon part of PFOA molecules to adsorb. Simulations show that the interaction of PFOA tails with fluorinated linkers is more favorable than upon insertion of a PFOA tail inside the  $\beta$ -CD cavity and formation of  $\beta$ -CD-PFOA host-guest complexes as was originally assumed for these networks. We demonstrate that the combination of these interactions is important to simultaneously achieve effective adsorption and selectivity of the network toward PFOA. The network with fluorinated linkers provides a 3-fold higher adsorption efficiency for the PFOA pollutant compared to its hydrogenated counterpart ammonium octanoate, confirming the preferential interaction toward fluorinated surfactants. The synergistic effect from electrostatic and hydrophobic interactions of surfactants with CD and specific linkers is the key mechanism for efficient PFOA adsorption as observed in our simulations as well as being consistent with experimental observations.<sup>38</sup> Note, however, that it does not mean that inclusion of fluorinated linkers is a must for efficient PFOA (or PFAS) adsorption. For example, linkers with amine functional groups can serve the same role as adsorbed ammonium counterions in our system, i.e., effectively interact with the anionic headgroup of the pollutant. Experimental evidence for efficient adsorption of PFAS on CD networks with nonfluorinated linkers has been reported.<sup>35</sup> Our simulations demonstrate how one can elucidate the contributions of each component of the CD-based network (or in principle any polymeric network) in the adsorption of PFAS pollutants and utilize molecular scale insight for the efficient design and optimization of the next-generation of PFAS adsorbents.

# ASSOCIATED CONTENT

## Supporting Information

The Supporting Information is available free of charge at https://pubs.acs.org/doi/10.1021/acsmaterialslett.2c00168.

Description and parameters of force field and system setup, description of analysis methods, and additional radial distribution functions, snapshots, and distribution profiles for simulated systems (PDF)

### AUTHOR INFORMATION

## **Corresponding Author**

Dmitry Bedrov — Department Materials Science and Engineering, University of Utah, Salt Lake City, Utah 84112, United States; orcid.org/0000-0002-3884-3308; Email: d.bedrov@utah.edu

# Authors

Aditya Choudhary — Department Materials Science and Engineering, University of Utah, Salt Lake City, Utah 84112, United States

Dengpan Dong — Department Materials Science and Engineering, University of Utah, Salt Lake City, Utah 84112, United States; orcid.org/0000-0002-3381-3425

Marina Tsianou — Department of Chemical and Biological Engineering, University at Buffalo, The State University of New York (SUNY), Buffalo, New York 14260-4200, United States; © orcid.org/0000-0003-3340-627X

Paschalis Alexandridis – Department of Chemical and Biological Engineering, University at Buffalo, The State University of New York (SUNY), Buffalo, New York 14260-4200, United States; orcid.org/0000-0001-6989-8232

Complete contact information is available at: https://pubs.acs.org/10.1021/acsmaterialslett.2c00168

### **Notes**

The authors declare no competing financial interest.

### ACKNOWLEDGMENTS

This research was funded by the U.S. National Science Foundation (NSF), grant numbers CBET-1930935 and CBET-1930959.

### REFERENCES

- (1) Castiglioni, S.; Valsecchi, S.; Polesello, S.; Rusconi, M.; Melis, M.; Palmiotto, M.; Manenti, A.; Davoli, E.; Zuccato, E. Sources and Fate of Perfluorinated Compounds in the Aqueous Environment and in Drinking Water of a Highly Urbanized and Industrialized Area in Italy. *J. Hazard. Mater.* **2015**, 282, 51–60.
- (2) Ng, C. A.; Hungerbühler, K. Bioaccumulation of Perfluorinated Alkyl Acids: Observations and Models. *Environ. Sci. Technol.* **2014**, *48*, 4637–4648.
- (3) Kudo, N.; Kawashima, Y. Toxicity and Toxicokinetics of Perfluorooctanoic Acid in Humans and A Nimals. *J. Toxicol. Sci.* **2003**, 28, 49–57.
- (4) Barry, V.; Winquist, A.; Steenland, K. Perfluorooctanoic Acid (PFOA) Exposures and Incident Cancers among Adults Living near a Chemical Plant. *Environ. Health Perspect.* **2013**, *121*, 1313–1318.
- (5) Braun, J. M.; Chen, A.; Romano, M. E.; Calafat, A. M.; Webster, G. M.; Yolton, K.; Lanphear, B. P. Prenatal Perfluoroalkyl Substance Exposure and Child Adiposity at 8 Years of Age: The HOME Study. *Obesity* **2016**, *24*, 231–237.
- (6) Hu, X. C.; Andrews, D. Q.; Lindstrom, A. B.; Bruton, T. A.; Schaider, L. A.; Grandjean, P.; Lohmann, R.; Carignan, C. C.; Blum, A.; Balan, S. A.; Higgins, C. P.; Sunderland, E. M. Detection of Polyand Perfluoroalkyl Substances (PFASs) in U.S. Drinking Water Linked to Industrial Sites, Military Fire Training Areas, and Wastewater Treatment Plants. *Environ. Sci. Technol. Lett.* **2016**, 3, 344–350.
- (7) Barzen-Hanson, K. A.; Roberts, S. C.; Choyke, S.; Oetjen, K.; McAlees, A.; Riddell, N.; McCrindle, R.; Ferguson, P. L.; Higgins, C. P.; Field, J. A. Discovery of 40 Classes of Per- and Polyfluoroalkyl Substances in Historical Aqueous Film-Forming Foams (AFFFs) and AFFF-Impacted Groundwater. *Environ. Sci. Technol.* **2017**, *51*, 2047–2057.
- (8) PFAS Contamination of Drinking Water Far More Prevalent Than Previously Reported. https://www.ewg.org/research/national-pfastesting/ (accessed 2020-09-02).
- (9) U.S. EPA. Drinking Water Health Advisories for PFOA and PFOS. 2016; No. November, pp 1-4.
- (10) Trojanowicz, M.; Bojanowska-Czajka, A.; Bartosiewicz, I.; Kulisa, K. Advanced Oxidation/Reduction Processes Treatment for Aqueous Perfluorooctanoate (PFOA) and Perfluorooctanesulfonate (PFOS) A Review of Recent Advances. *Chem. Eng. J.* **2018**, 336, 170–199.
- (11) Yamamoto, T.; Noma, Y.; Sakai, S. I.; Shibata, Y. Photo-degradation of Perfluorooctane Sulfonate by UV Irradiation in Water and Alkaline 2-Propanol. *Environ. Sci. Technol.* **2007**, *41*, 5660–5665.
- (12) Lin, H.; Niu, J.; Ding, S.; Zhang, L. Electrochemical Degradation of Perfluorooctanoic Acid (PFOA) by Ti/SnO2-Sb, Ti/SnO2-Sb/PbO2 and Ti/SnO2-Sb/MnO2 Anodes. *Water Res.* **2012**, *46*, 2281–2289.
- (13) Hori, H.; Hayakawa, E.; Einaga, H.; Kutsuna, S.; Koike, K.; Ibusuki, T.; Kiatagawa, H.; Arakawa, R. Decomposition of Environmentally Persistent Perfluorooctanoic Acid in Water by Photochemical Approaches. *Environ. Sci. Technol.* **2004**, *38*, 6118–6124.

- (14) Ochoa-Herrera, V.; Sierra-Alvarez, R. Removal of Perfluorinated Surfactants by Sorption onto Granular Activated Carbon, Zeolite and Sludge. *Chemosphere* **2008**, *72*, 1588–1593.
- (15) Alves, A. V.; Tsianou, M.; Alexandridis, P. Fluorinated Surfactant Adsorption on Mineral Surfaces: Implications for PFAS Fate and Transport in the Environment. *Surfaces* **2020**, *3*, 516–566.
- (16) Deng, S.; Yu, Q.; Huang, J.; Yu, G. Removal of Perfluorooctane Sulfonate from Wastewater by Anion Exchange Resins: Effects of Resin Properties and Solution Chemistry. *Water Res.* **2010**, *44*, 5188–5195.
- (17) Sini, K.; Bourgeois, D.; Idouhar, M.; Carboni, M.; Meyer, D. Metal-Organic Framework Sorbents for the Removal of Perfluorinated Compounds in an Aqueous Environment. *New J. Chem.* **2018**, 42, 17889–17894.
- (18) Karoyo, A. H.; Wilson, L. D. Investigation of the Adsorption Processes of Fluorocarbon and Hydrocarbon Anions at the Solid-Solution Interface of Macromolecular Imprinted Polymer Materials. *J. Phys. Chem. C* **2016**, *120*, 6553–6568.
- (19) Eschauzier, C.; Beerendonk, E.; Scholte-Veenendaal, P.; De Voogt, P. Impact of Treatment Processes on the Removal of Perfluoroalkyl Acids from the Drinking Water Production Chain. *Environ. Sci. Technol.* **2012**, *46*, 1708–1715.
- (20) Du, Z.; Deng, S.; Bei, Y.; Huang, Q.; Wang, B.; Huang, J.; Yu, G. Adsorption Behavior and Mechanism of Perfluorinated Compounds on Various Adsorbents-A Review. *J. Hazard. Mater.* **2014**, 274. 443–454.
- (21) Ching, C.; Klemes, M. J.; Trang, B.; Dichtel, W. R.; Helbling, D. E.  $\beta$ -Cyclodextrin Polymers with Different Cross-Linkers and Ion-Exchange Resins Exhibit Variable Adsorption of Anionic, Zwitterionic, and Nonionic PFASs. *Environ. Sci. Technol.* **2020**, *54*, 12693–12702.
- (22) Shetty, D.; Jahović, I.; Skorjanc, T.; Erkal, T. S.; Ali, L.; Raya, J.; Asfari, Z.; Olson, M. A.; Kirmizialtin, S.; Yazaydin, A. O.; Trabolsi, A. Rapid and Efficient Removal of Perfluorooctanoic Acid from Water with Fluorine-Rich Calixarene-Based Porous Polymers. ACS Appl. Mater. Interfaces 2020, 12, 43160–43166.
- (23) Kumarasamy, E.; Manning, I. M.; Collins, L. B.; Coronell, O.; Leibfarth, F. A. Ionic Fluorogels for Remediation of Per-and Polyfluorinated Alkyl Substances from Water. *ACS Cent. Sci.* **2020**, *6*, 487–492.
- (24) Ateia, M.; Arifuzzaman, M.; Pellizzeri, S.; Attia, M. F.; Tharayil, N.; Anker, J. N.; Karanfil, T. Cationic Polymer for Selective Removal of GenX and Short-Chain PFAS from Surface Waters and Wastewaters at Ng/L Levels. *Water Res.* **2019**, *163*, 114874.
- (25) Zheng, Z.; Yu, H.; Geng, W. C.; Hu, X. Y.; Wang, Y. Y.; Li, Z.; Wang, Y.; Guo, D. S. Guanidinocalix[5] Arene for Sensitive Fluorescence Detection and Magnetic Removal of Perfluorinated Pollutants. *Nat. Commun.* **2019**, *10*, 1–9.
- (26) Omorodion, H.; Palenzuela, M.; Ruether, M.; Twamley, B.; Platts, J. A.; Baker, R. J. A Rationally Designed Perfluorinated Host for the Extraction of PFOA from Water Utilising Non-Covalent Interactions. *New J. Chem.* **2018**, 42, 7956–7968.
- (27) Lan, S.; Zhan, S.; Ding, J.; Ma, J.; Ma, D. Pillar[n]Arene-Based Porous Polymers for Rapid Pollutant Removal from Water. *J. Mater. Chem. A* **2017**, *5*, 2514–2518.
- (28) Weiss-Errico, M. J.; O'Shea, K. E. Detailed NMR Investigation of Cyclodextrin-Perfluorinated Surfactant Interactions in Aqueous Media. *J. Hazard. Mater.* **2017**, 329, 57–65.
- (29) Guo, W.; Fung, B. M.; Christian, S. D. NMR Study of Cyclodextrin Inclusion of Fluorocarbon Surfactants in Solution. *Langmuir* **1992**, *8*, 446–451.
- (30) Karoyo, A. H.; Borisov, A. S.; Wilson, L. D.; Hazendonk, P. Formation of Host-Guest Complexes of  $\beta$ -Cyclodextrin and Perfluorooctanoic Acid. *J. Phys. Chem. B* **2011**, *115*, 9511–9527.
- (31) Alsbaiee, A.; Smith, B. J.; Xiao, L.; Ling, Y.; Helbling, D. E.; Dichtel, W. R. Rapid Removal of Organic Micropollutants from Water by a Porous  $\beta$ -Cyclodextrin Polymer. *Nature* **2016**, *529*, 190–194.
- (32) Xiao, L.; Ling, Y.; Alsbaiee, A.; Li, C.; Helbling, D. E.; Dichtel, W. R.  $\beta$ -Cyclodextrin Polymer Network Sequesters Perfluorooctanoic

- Acid at Environmentally Relevant Concentrations. J. Am. Chem. Soc. 2017, 139, 7689–7692.
- (33) Ling, Y.; Klemes, M. J.; Xiao, L.; Alsbaiee, A.; Dichtel, W. R.; Helbling, D. E. Benchmarking Micropollutant Removal by Activated Carbon and Porous  $\beta$ -Cyclodextrin Polymers under Environmentally Relevant Scenarios. *Environ. Sci. Technol.* **2017**, *51*, 7590–7598.
- (34) Xiao, L.; Ching, C.; Ling, Y.; Nasiri, M.; Klemes, M. J.; Reineke, T. M.; Helbling, D. E.; Dichtel, W. R. Cross-Linker Chemistry Determines the Uptake Potential of Perfluorinated Alkyl Substances by  $\beta$ -Cyclodextrin Polymers. *Macromolecules* **2019**, *52*, 3747–3752.
- (35) Klemes, M. J.; Skala, L. P.; Ateia, M.; Trang, B.; Helbling, D. E.; Dichtel, W. R. Polymerized Molecular Receptors as Adsorbents to Remove Micropollutants from Water. *Acc. Chem. Res.* **2020**, *53*, 2314–2324.
- (36) Klemes, M. J.; Ling, Y.; Chiapasco, M.; Alsbaiee, A.; Helbling, D. E.; Dichtel, W. R. Phenolation of Cyclodextrin Polymers Controls Their Lead and Organic Micropollutant Adsorption. *Chem. Sci.* **2018**, 9, 8883–8889.
- (37) Yang, A.; Ching, C.; Easler, M.; Helbling, D. E.; Dichtel, W. R. Cyclodextrin Polymers with Nitrogen-Containing Tripodal Crosslinkers for Efficient PFAS Adsorption. *ACS Mater. Lett.* **2020**, *2*, 1240–1245.
- (38) Ching, C.; Ling, Y.; Trang, B.; Klemes, M.; Xiao, L.; Yang, A.; Barin, G.; Dichtel, W. R.; Helbling, D. E. Identifying the Physicochemical Properties of  $\beta$ -Cyclodextrin Polymers That Determine the Adsorption of Perfluoroalkyl Acids. *Water Res.* **2022**, 209, 117938.
- (39) Bedrov, D.; Piquemal, J.-P.; Borodin, O.; MacKerell, A. D.; Roux, B.; Schröder, C. Molecular Dynamics Simulations of Ionic Liquids and Electrolytes Using Polarizable Force Fields. *Chem. Rev.* **2019**, *119*, 7940–7995.
- (40) Dong, D.; Kancharla, S.; Hooper, J.; Tsianou, M.; Bedrov, D.; Alexandridis, P. Controlling the Self-Assembly of Perfluorinated Surfactants in Aqueous Environments. *Phys. Chem. Chem. Phys.* **2021**, 23, 10029–10039.
- (41) Kancharla, S.; Dong, D.; Bedrov, D.; Tsianou, M.; Alexandridis, P. Structure and Interactions in Perfluorooctanoate Micellar Solutions Revealed by Small-Angle Neutron Scattering and Molecular Dynamics Simulations Studies: Effect of Urea. *Langmuir* **2021**, *37*, 5339–5347.
- (42) Kancharla, S.; Choudhary, A.; Davis, R. T.; Dong, D.; Bedrov, D.; Tsianou, M.; Alexandridis, P. GenX in Water: Interactions and Self-Assembly. *J. Hazard. Mater.* **2022**, 428, 128137.
- (43) Palmer, B. J. Direct Application of Shake to the Velocity Verlet Algorithm. *J. Comput. Phys.* **1993**, *104*, 470–472.
- (44) Harada, K.; Xu, F.; Ono, K.; Iijima, T.; Koizumi, A. Effects of PFOS and PFOA on L-Type Ca2+ Currents in Guinea-Pig Ventricular Myocytes. *Biochem. Biophys. Res. Commun.* **2005**, 329, 487–494.
- (45) Karoyo, A. H.; Sidhu, P.; Wilson, L. D.; Hazendonk, P. Characterization and Dynamic Properties for the Solid Inclusion Complexes of  $\beta$ -Cyclodextrin and Perfluorobutyric Acid. *J. Phys. Chem. C* **2013**, *117*, 8269–8282.
- (46) Zhang, H.; Hogen-Esch, T. E.; Boschet, F.; Margaillan, A. Complex Formation of  $\beta$ -Cyclodextrin- and Perfluorocarbon-Modified Water-Soluble Polymers. *Langmuir* **1998**, *14*, 4972–4977.
- (47) Klemes, M. J.; Ling, Y.; Ching, C.; Wu, C.; Xiao, L.; Helbling, D. E.; Dichtel, W. R. Reduction of a Tetrafluoroterephthalonitrile- $\beta$ -Cyclodextrin Polymer to Remove Anionic Micropollutants and Perfluorinated Alkyl Substances from Water. *Angew. Chemie Int. Ed.* **2019**, *58*, 12049–12053.
- (48) Yan, B.; Munoz, G.; Sauvé, S.; Liu, J. Molecular Mechanisms of Per- and Polyfluoroalkyl Substances on a Modified Clay: A Combined Experimental and Molecular Simulation Study. *Water Res.* **2020**, *184*, 116166.
- (49) Wang, L.; Gong, X.; Wang, R.; Gan, Z.; Lu, Y.; Sun, H. Application of an Immobilized Ionic Liquid for the Passive Sampling of Perfluorinated Substances in Water. *J. Chromatogr. A* **2017**, *1515*, 45–53.